MOLECULAR ECOLOGY

Molecular Ecology (2017) **26**, 3276–3294 doi: 10.1111/mec.14092

Warm–cold colonization: response of oaks to uplift of the Himalaya–Hengduan Mountains

HONG-HU MENG,*† ‡ TAO SU,* XIAO-YANG GAO,§ JIE LI,† XIAO-LONG JIANG,¶ HANG SUN** and ZHE-KUN ZHOU***

*Key Laboratory of Tropical Forest Ecology, Xishuangbanna Tropical Botanical Garden, Chinese Academy of Sciences, Mengla 666303, China, †Center for Integrative Conservation, Xishuangbanna Tropical Botanical Garden, Chinese Academy of Sciences, Kunming 650223, China, ‡University of Chinese Academy of Sciences, Beijing 100049, China, §Key Laboratory of Tropical Plant Resources and Sustainable Use, Xishuangbanna Tropical Botanical Garden, Chinese Academy of Sciences, Mengla 666303, China, ¶Shanghai Chenshan Plant Science Research Center, Chinese Academy of Sciences, Shanghai 201602, China, **Key Laboratory for Plant Diversity and Biogeography of East Asia, Kunming Institute of Botany, Chinese Academy of Sciences, Kunming 650204, China

Abstract

Clarifying the relationship between distribution patterns of organisms and geological events is critical to understanding the impact of environmental changes on organismal evolution. *Quercus* sect. *Heterobalanus* is now distributed across the Himalaya–Hengduan Mountains (HHM) and warm lowland in East China, yet how the distribution patterns of this group changed in response to the HHM uplift remains largely unknown. This study examines the effect of tectonic events in the HHM region on the oaks, providing a biological perspective on the geological history of this region. Fifty-six populations of *Quercus* sect. *Heterobalanus* were genotyped using four chloroplast DNA regions and nine nuclear simple sequence repeat loci to assess population structure and diversity, supplemented by molecular dating and ancestral area reconstructions. The underlying demographic dynamics were compared using ecological niche models of the species distributions during the last glacial maximum and the present. These analyses illustrate that *Quercus* sect. *Heterobalanus* diversified as the HHM uplifted and climatic cooling during the mid-Miocene, colonizing the cold habitats from warm broadleaf mixed forests. Lineages in cold highlands and warm lowlands have diverged as a consequence of local adaptation to diverging climates since the late Miocene. Our results suggest that continuous uplift of the HHM in the late Miocene to early Pliocene accompanied by simultaneous cooling triggered the differentiation of oaks. The biogeography of *Quercus* sect. *Heterobalanus* illuminates the geological events responsible for the modern-day HHM.

Keywords: ancestral area reconstruction, colonization, ecological niche modelling, geological evolution, Himalaya–Hengduan Mountains, phylogeography, *Quercus* sect. *Heterobalanus*

Received 17 January 2016; revision received 14 February 2017; accepted 24 February 2017

Introduction

It is not difficult to be impressed by the grandeur of the Himalaya–Hengduan Mountains (HHM) and the rich biodiversity it hosts, but it is difficult to reconstruct how its biodiversity and elevation evolved. The Himalayas is the southern frontier of the Qinghai-Tibetan Plateau (QTP, including the Tibetan plateau, Himalayas, Hengduan Mountains, etc.), whereas the Hengduan Mountains is the southeastern margin of the QTP (Zhang *et al.* 2002). Undoubtedly, the collision between India and Eurasia during the Cenozoic has produced uplift of the plateau, which was the most substantial active orogeny in Asia, maybe even on the earth (Yin & Harrison 2000; Royden *et al.* 2008; Lippert *et al.*

Correspondence: Zhe-Kun Zhou, Fax: +86 871 65160916; E-mail: zhouzk@xtbg.ac.cn

2014). As one of the planet's most imposing geomorphological features, the HHM has played an important role in the evolution of the flora and fauna in this region. The HHM, as a significant reservoir of global biodiversity hot spots in general (Myers *et al.* 2000), where occupy one of the most important biodiversity in the world. Therefore, the evolutionary history and adaptation of plants on these regions are of particular interest (Liu *et al.* 2014; Wen *et al.* 2014). However, details of the geological events underlying uplift of the QTP region, especially the correlations between geological evolution and biological response in the HHM, are still debated nowadays (Harrison *et al.* 1992; Yin & Harrison 2000; Tapponnier *et al.* 2001; Mulch & Chamberlain 2006; Royden *et al.* 2008; Lippert *et al.* 2014; Favre *et al.* 2015; Li *et al.* 2015; Renner 2016; Ding *et al.* 2017). Accordingly, quantifying these tectonic features of the HHM uplift and the response of organisms to the orogenic process are of great interest and challenging to geologists and biologists alike.

Uplift in the plateau and crustal movements have caused large-scale changes in air circulation patterns, climatic zones, large river drainages and vegetation (Li & Fang 1999). In addition to the uplift, its associated orogenic and environmental effects have likely served as a major force in speciation, origin of genetic discontinuities and organism evolution throughout the QTP region (Che *et al.* 2010; Favre *et al.* 2015; Zhao *et al.* 2015). During the late Oligocene to early Miocene, the uplift of the plateau caused the disappearance of tropical/subtropical evergreen broadleaved forest in the QTP as it reached higher altitude (Wu *et al.* 2007; Ding *et al.* 2017). The Miocene cooling coincident with the Cenozoic uplift of the plateau is supported by the geological records of the Tibetan region (George *et al.* 2001). The evergreen broadleaved forest and the sclerophyllous forests which was derived from Tethyan vegetation and dominated by sclerophyllous plants is still the typical vegetation of the QTP (Takhtajan 1969; Axelrod 1975; Wu *et al.* 1987).

The biodiversity of the HHM has traditionally been explained that the lowlands of the Himalayas and Hengduan Mountains provide refugia for plants throughout climatic oscillations and glaciation in the Quaternary (Qiu *et al.* 2011). However, few current hypotheses emphasize the role of historical and evolutionary factors in shaping plant diversity before the Quaternary. For example, some studies of plant species considered events occurring further back to elucidate pre-Quaternary population dynamics in the HHM; these efforts have found clear imprints of the region's Neogene history in patterns of within-species diversity that are consistent with the formation of major genetic lineages as a consequence of the uplift (e.g. Wang *et al.* 2010; Xu *et al.* 2010; Jia *et al.* 2012; Li *et al.* 2013). Accordingly, we expect the evolutionary history of the plant taxa distributed across the HHM and the warm lowlands in East China to exhibit the evolutionary responses to geological events, and in turn, to illuminate the geological evolution of the HHM from a biological perspective.

Quercus sect. *Heterobalanus*, a section of sclerophyllous oaks in high elevation of East Asia, are mainly distributed in the HHM and the mountain tops of East China. This section is considered a monophyletic group based on the taxonomical and evolutionary implications of leaf anatomy and architecture of *Quercus* (Zhou *et al.* 1994). In the HHM region, the most abundant sclerophyllous oaks are *Quercus* sect. *Heterobalanus*. More recently, fossils of this section have been reported from the Neogene in the HHM and adjacent regions (Zhou *et al.* 2003; He *et al.* 2014; Su *et al.* 2015; Huang *et al.* 2016). The oldest-known fossil of this section was discovered in Namulin, southern Tibet (Fig. 1; Li & Guo 1976), and the age of the stratum containing the specimen has been constrained to the middle Miocene, *ca.* 15 Ma (Spicer *et al.* 2003). The fossils of *Quercus semecarpifolia* unearthed from the northern slope in Xixiabangma were used to estimate the elevation of the Himalayas (Hsu *et al.* 1973), which was considered the first paleoecological evidence of the uplift of the Himalayas from plant fossils (Li *et al.* 2015). Later, these fossils were used to explain the uplift of the Himalayas from different approaches (Hsu *et al.* 1973; Zhou *et al.* 2003, 2007). Thus, the high quality of the fossil record and present distribution in the HHM region and eastern China indicate that *Quercus* sect. *Heterobalanus* is an ideal model for inferring the evolutionary response to both the geological and environmental changes of the HHM as well as the other regions. Given that most species that have ever existed on earth are extinct, it stands to reason that the evolutionary history can be better understood with fossil taxa (Meng *et al.* 2014). Therefore, this study system is particularly amenable to trace evolutionary history and calibrate molecular dating for the reliable fossil evidence is the best approach of calibrating divergence times in molecular analyses.

There are seven species of *Quercus* sect. *Heterobalanus* listed in *Flora of China* (Huang *et al.* 1999; i.e., *Quercus semecarpifolia*, *Q. guajavifolia*, *Q. aquifolioides*, *Q. rehderiana*, *Q. spinosa*, *Q. monimotricha* and *Q. senescens*), which are mainly distributed in the HHM, and scattered among the high mountain tops of East China (Fig. 1). The Hengduan Mountains is a biodiversity centre of *Quercus* sect. *Heterobalanus* as they exhibit a wide distribution and large species numbers in the area, which has been supported by rich fossil records from the

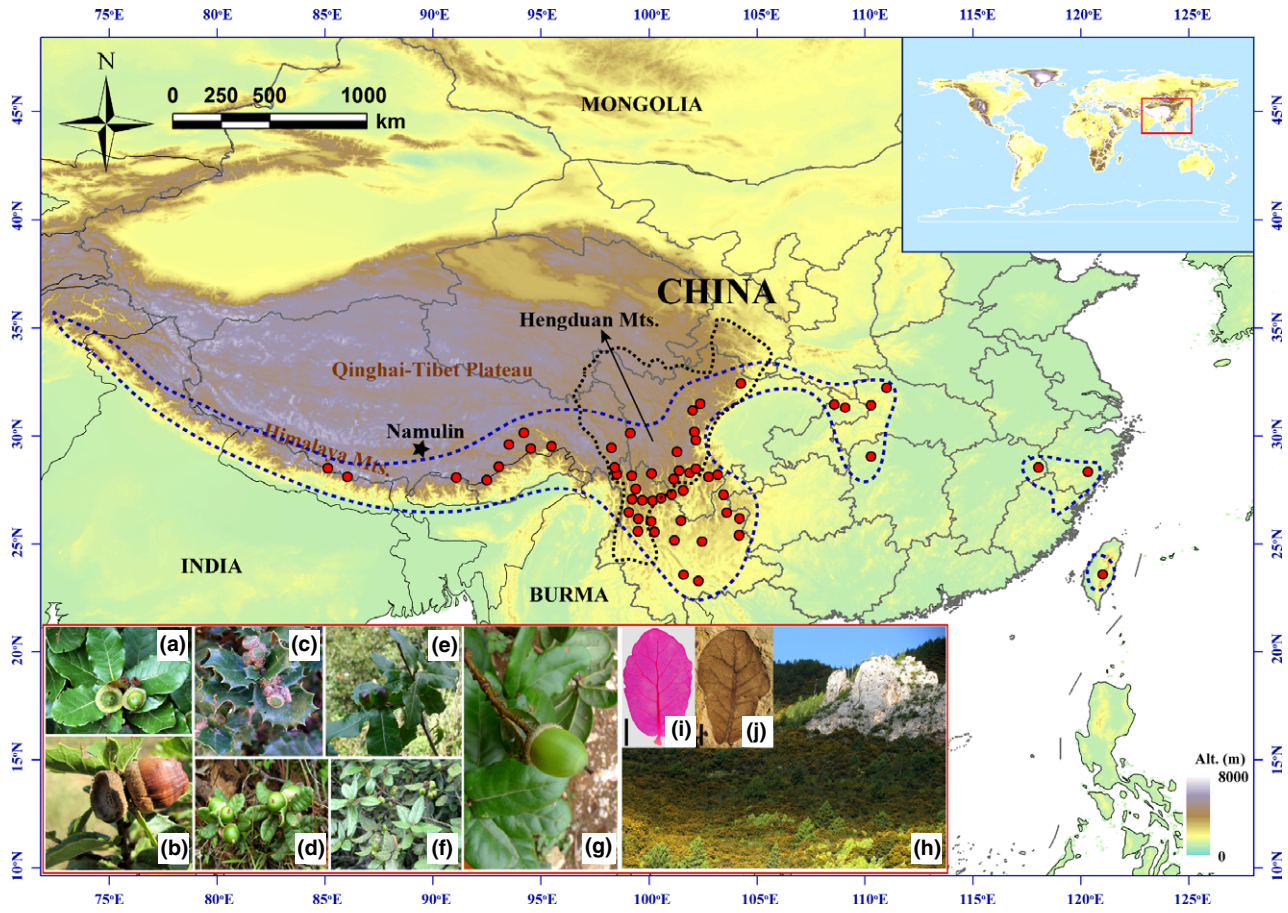

Fig. 1 Geographic distribution of *Quercus* sect. *Heterobalanus*. Blue dashed lines denote the geographic distribution areas of *Quercus* sect. *Heterobalanus*; black dashed lines denote the Hengduan Mountains; red dots denote the materials collection sites; and the star denotes where the oldest known fossils of this section reported, Namulin. (a) *Q. guajavifolia*, (b) *Q. rehderiana*, (c) *Q. aquifolioides*, (d) *Q. monimotricha*, (e) *Q. semecarpifolia*, (f) *Q. senescens*, (g) *Q. spinosa*, (h) the habitats of *Quercus* sect. *Heterobalanus*, (i) the leaf architecture of *Quercus* sect. *Heterobalanus*, scale bar = 1 cm, and (j) the leaf fossil of *Quercus* sect. *Heterobalanus*, scale bar = 1 cm.

mid-Miocene to the Pleistocene in the HHM and adjacent regions (Zhou *et al.* 2007; He *et al.* 2014; Huang *et al.* 2016). Phylogeographic research also provides evidence that the Hengduan Mountains is a distribution centre for *Q. aquifolioides* (Du *et al.* 2016). The distinctive distribution patterns span the HHM and eastern China, as well as the accurate fossil records (Fig. 1), and provide an exceptional opportunity to elucidate the processes by which biodiversity increased as a result of the formation of the HHM, and the uplifting processes itself. Thus, it offers a unique model to disentangle the evolutionary processes underlying botanical evolution in the important biodiversity hot spot.

Here, this phylogeographic objective using molecular dating, ecological niche modelling (ENM), ancestral range reconstructions, as well as the relative geological events, which enable us to (i) elucidate the role of the orogenic processes that created the HHM in shaping the geographic distribution of plants in the surrounding region; and in turn, to (ii) illuminate the geological history of the HHM from a biological perspective.

Materials and methods

Taxa sampling

A total of 529 foliar samples of *Quercus* sect. *Heterobalanus* were collected from 56 populations at elevations between 1034 m and 4236 m (Fig. 1, Table 1). The samples included all recognized species of *Quercus* sect. *Heterobalanus* according to *Flora of China* (Huang *et al.* 1999), and the sampling scale covered almost all distribution ranges. All sampled in-group species and locations are listed in Table 1, and the geographic distribution is depicted in Fig. 1. Chloroplast DNA (cpDNA) sequence variation and nuclear microsatellite (nSSR) analyses were performed using genetic material from each sample collected.

Table 1 Details of *Quercus* sect. *Heterobalanus* populations used in the study, sample sizes (*n*) and cpDNA haplotypes (*H*) observed

Species	Collection site	Geographical coordinates, altitude	Code	*n*	*H*
Q. aquifolioides	Lanping, Nujiang, Yunnan	N 26°45.74, E 99°07.34; 3027 m	D01	11	H8
	Zhongdian Botanical Garden, Shangri-La, Yunnan	N 26°54.01, E 99°37.57; 3332 m	D02	10	H7
	Rumei, Markam, Tibet	N 29°44.46, E 98°26.24; 3929 m	Z02	10	H6
	Songduo, Batang, Sichuan	N 30°11.59, E 99°13.23; 2987 m	C01	9	H6
	Songgui, Dengchuan, Dali, Yunnan	N 26°04.57, E 100°09.37; 2508 m	D09	8	H7
	Xinyingpan, Ninglang, Yunnan	N 27°11.79, E 100°53.83; 2473 m	D11	10	H7
Q. guajavifolia	Dongzhulin Monastery, Benzilan, Deqin, Yunnan	N 28°14.36, E 99°18.05; 2837 m	D06	10	H7
	Baima Snow Mts., Deqin, Yunnan	N 28°22.02, E 98°51.92; 3832 m	D05	9	H7
	Yading, Daocheng, Sichuan	N 28°24.74, E 100°11.14; 4163 m	C02	10	H17
	Hongla Mts., Yanjing, Markam, Tibet	N 25°54.86, E 98°40.79; 4236 m	Z01	10	H6
	Yulong Snow Mts., Lijiang, Yunnan	N 27°01.03, E 100°15.40; 2703 m	D01	10	H8
	Gongga Mts., Kangding, Sichuan	N 29°24.83, E 101°28.29; 3784 m	C08	6	H17
	Mosuo Revier, Barkam, Aba, Sichuan	N 31°50.38, E 102°36.07; 2727 m	C13	9	H28
	Zhahui, Longzi, Tibet	N 28°46.35, E 93°04.15; 2759 m	Z03	9	H3
	Jiuka Monastery, Lakang, Luozha, Tibet	N 28°05.59, E 91°07.42; 4230 m	Z04	13	H3
	Lebugu Mts., Cuona, Tibet	N 27°94.99, E 92°49.11; 3526 m	Z05	14	H3
	Liantie, Eryuan, Yunan	N 25°58.95, E 99°48.41; 2009 m	D12	12	H9
	Eastern suburbs of Bomi, Tibet	N 29°50.87, E 95°48.40; 3413 m	Z06	10	H5
	Yigong, Tongmai, Tibet	N 30°13.46, E 94°52.09; 2745 m	Z07	10	H5
	Western suburbs of Nyingchi, Tibet	N 29°41.70, E 94°20.86; 3074 m	Z08	10	H4
	Jinda, Gongbujiangda, Tibet	N 29°58.33, E 93°51.77; 3930 m	Z09	10	H4
	Mopan Mts., Xinping, Yunnan	N 23°56.26, E 101°59.20; 2506 m	D21	12	H13
Q. semecarpifolia	Zhangmu Port, Nyalam, Tibet	N 28°10.20, E 86°05.72; 2046 m	Z10	11	H2
	Jilong Town, Jilong, Tibet	N 28°50.03, E 85°13.22; 2607 m	Z11	11	H1
Q. rehderiana	Chongjiang River, Lijiang, Yunnan	N 27°01.84, E 99°69.93; 2513 m	D07	8	H11
	Junzi Mts., Nanhua, Yunnan	N 25°17.28, E 101°16.05; 2086 m	D08	10	H12
	Meiyu Town, Yanyuan, Sichuan	N 27°28.47, E 101°02.59; 2403 m	C03	10	H16
	Shuiluo Town, Muli, Sichuan	N 27°59.87, E 101°12.51; 2453 m	C04	10	H16
	Wulaxi, Jiulong, Sichuan	N 28°38.50, E 101°38.39; 2007 m	C07	9	H18
	Weicheng, Yanyuan, Sichuan	N 27°47.96, E 101°57.03; 2258 m	C05	9	H16
	Erlang Mts., Tianquan, Sichuan	N 29°50.39, E 102°15.44; 2174 m	C15	8	H27
	Xide, Sichuan	N 28°09.63, E 102°74.51; 1685 m	C10	10	H21
	Toll gate of Sichuan-Yunnan, Yongren, Yunnan	N 26°08.05, E 101°17.14; 2015 m	D14	2	H15
	Xiaoshao, Kunming, Yunnan	N 25°11.49, E 102°44.29; 2275 m	D15	12	H14
	Wuliping, Longchang, Xuanwei, Yunnan	N 26°18.35, E 104°17.76; 2144 m	D16	6	H24
	Heishitou, Weining, Guizhou	N 26°45.01, E 103°58.55; 2363 m	Q01	9	H24
	Jizu Mts., Binchuan, Yunnan	N 25°55.55, E 100°23.86; 1838 m	D13	12	H10
Q. spinosa	Sanhe, Kangding, Sichuan	N 30°19.29, E 102°09.35; 1714 m	C11	10	H27
	Badi, Danba, Sichuan	N 31°17.40, E 102°01.20; 2116 m	C12	10	H28
	Muzuo, Pingwu, Sichuan	N 32°42.22, E 104°24.11; 1683 m	C14	10	H29
	Houpig, Chengkou, Chongqing	N 31°46.06, E 108°57.23; 2144 m	Y01	7	H30
	Hongchiba, Wuxi, Chongqing	N 31°30.77, E 109°07.33; 1513 m	Y02	10	H30
	Tianmen Mts., Zhangjiajie, Hunan	N 29°03.59, E 110°28.59; 1479 m	X01	10	H30
	Tianmenya, Shennongjia, Hubei	N 31°43.37, E 110°28.10; 1806 m	E01	6	H30
	Wudang Mts., Shiyan, Hubei	N 32°24.20, E 111°00.22; 1364 m	E02	9	H30
	Sanqing Mts., Yushan, Jiangxi	N 28°54.22, E 118°03.24; 1541 m	G01	3	H30
	Longtantou, Danzhu, Xianju, Zhejiang	N 28°33.56, E 120°32.15; 1034 m	M01	2	H30
	Yushan, Nantou, Taiwan	N 23°59.24, E 121°01.32; 3150 m	T01	10	H31
	Dalengshan Mts., Shiping, Yunan	N 23°27.18, E 102°28.53; 2314 m	D20	11	H14
Q. monimotricha	Laojunshan Mts., Jianchuan, Yunnan	N 26°16.51, E 99°49.48; 2411 m	D03	12	H8
	Huilong, Mianning, Sichuan	N 28°28.56, E 101°86.47; 1842 m	C06	11	H19, H20
	Jingan, Zhaotong, Yunnan	N 27°28.38, E 103°43.58; 2164 m	D19	11	H23
Q. senescens	Yongchun, Weixi, Yunnan	N 27°07.81, E 99°20.51; 2421 m	D02	12	H7
	Tuowu, Miangning, Sichuan	N 28°87.04, E 102°15.47; 2157 m	C09	10	H21
	Niulanjiang, Songming, Yunnan	N 28°19.53, E 103°16.09; 2182 m	D17	10	H22
	Zhongtian, Fuyuan, Yunnan	N 25°40.58, E 104°16.20; 1985 m	D18	6	H25, H26

Laboratory protocols

Total genomic DNA of all samples was extracted using the Plant Genomic DNAKit (Tiangen Biotech, Beijing, China) according to the manufacturer's protocol. Four cpDNA regions were sequenced from each DNA extraction: *psb*A–*trn*H, a portion of the *psb*A region (Sang *et al.* 1997) and the *trn*H region (Fazekas *et al.* 2010); *rps*16 (Oxelman *et al.* 1997); *trn*S–*trn*G (Hamilton 1999); and *rpl*32–*trn*L (Shaw *et al.* 2007). Because cpDNA is maternally inherited, haploid and nonrecombining, these sequences were concatenated for each individual prior to subsequent analyses. In addition, a total of nine nSSR loci were also amplified: ssrQrZAG30, ssrQrZAG96, ssrQrZAG112 (Kampfer *et al.* 1998); ssrQpZAG36, ssrQpZAG110, ssrQpZAG16 (Steinkellner *et al.* 1997); MSQ13(TC)n (Dow *et al.* 1995); and quru-GA-0C11, quru-GA-1C08 (Aldrich *et al.* 2002). The PCR mixtures for cpDNA amplification reactions were described for *Lagochilus* by Meng & Zhang (2011, 2013). The thermocycling conditions for PCR are given as follows: for *psb*A–*trn*H: 94 °C, 4 min; 35 × (94 °C, 30 s; 56 °C, 60 s; 72 °C, 1 min); and 72 °C 10 min. *rps*16: 95 °C, 2 min; 33 × (95 °C, 30 s; 56 °C, 60 s; 72 °C, 2 min); and 72 °C 10 min. *trn*S–*trn*G: 95 °C, 2 min; 30 × (94 °C, 30 s; 52 °C, 30 s; 72 °C, 90 s); and 72 °C 10 min. *rpl*32–*trn*L: 94 °C, 2 min; 30 × (94 °C, 30 s; 56 °C, 60 s; 72 °C, 2 min); and 72 °C 10 min. PCR products were purified using the QIAquick Gel Extraction Kit (Qiagen, Hilden, Germany). The same primers were used for sequencing in Sangon Biotech (Shanghai) Co., Ltd., China. All sequences are deposited in GenBank, and the Accession nos are KU245764–KU245923 and KY249208–KY249239. The protocols of nuclear simple sequence repeat (nSSR) were performed by Sangon Biotech (Shanghai). In the actions, PCR mixtures (a total volume of 25 μL) for nSSR amplification contained: 1 μL genomic DNA, 0.5 μL of each primer, 0.5 μL dNTP (10 mM), 2.5 μL *taq* buffer, 2.0 μL $MgCl_2$ (25 mM), 0.2 μL *taq* DNA-polymerase. The PCR amplifications were performed as follows: 95 °C, 3 min; 10 × (95 °C, 30 s; 60 °C, 30 s; 72 °C, 30 s); after that 20 × (95 °C, 30 s; 55 °C, 30 s; 72 °C, 30 s); and 72 °C, 6 min.

Data analyses

The cpDNA haplotypes (h), haplotype diversities (H_d) and nucleotide diversities (π) were determined using DNASP v5.1 (Librado & Rozas 2009). G_{ST} and N_{ST} were assessed in HAPLONST and PERMUT to estimate differentiation between populations with unordered and ordered alleles (G_{ST} and N_{ST}, respectively) based on 1000 random permutations (Pons & Petit 1996). N_{ST} was compared to G_{ST} using U-statistics to indicate the presence of phylogeographic structure (i.e. when $N_{ST} > G_{ST}$). The evolutionary relationships among the haplotypes were inferred using a median-joining network implemented in NETWORK v2.0 (Bandelt *et al.* 1999). A spatial analysis of molecular variance (SAMOVA) was implemented to define the number of groups (K) that are geographically homogenous and maximally differentiated from each other (Dupanloup *et al.* 2002). Additionally, an analysis of molecular variance (AMOVA) was performed to examine the genetic variation within and among populations according to the number of groups (K) according to SAMOVA using ARLEQUIN v3.0 (Excoffier *et al.* 2005). Selective neutrality (Tajima's D; Fu's F_S) was tested to infer potential population growth and expansion (Tajima 1989; Fu 1997). For clades and subclades identified, the null hypothesis of spatial expansion was tested using a mismatch distribution analysis (MDA) in ARLEQUIN v3.0 (Excoffier *et al.* 2005). The goodness of fit was tested using the sum of squared deviations between observed and expected mismatch distributions as well as the raggedness index (HRag) across 1000 parametric bootstrap replicates (Harpending 1994).

Genetic subgroups in the nSSR data set were converted from Genepop to Structure format with CREATE v1.1 (Coombs *et al.* 2008). The repeatability of the results and convergence of the Markov chain Monte Carlo (MCMC) procedure were tested by carrying out a series of 10 replicate runs for each prior value of the number of clusters (K), set between 1 and 20 in STRUCTURE v2.3 (Pritchard *et al.* 2003). Each run consisted of a burn-in of 2×10^4 iterations, followed by 10^5 iterations. Two types of inference were performed using the admixture model of ancestry together with the correlated allele frequencies model (Falush *et al.* 2003), both with and without the use of sampling location as prior information (Hubisz *et al.* 2009). Two alternative methods were used to explore the true number of gene pools: first by monitoring the change in average of log-likelihood of the data, $\log_e P(D)$, of independent runs for each K and then by observing the second-order rate of change of $\log_e P(D)$ between successive K values (Evanno *et al.* 2005), which is based on the rate of change in the log-likelihood between successive K values. The results were confirmed by longer runs with K sets between 1 and 5, with 10 replicate runs at each K, 2×10^5 burn-in iterations, and 10^6 iterations. The results of structure analyses were visualized in DISTRUCT v1.0 (Rosenberg 2004). To quantify variation in nSSRs and cpDNA sequences among populations, AMOVA were performed in ARLEQUIN v3.0 using Φ- and R-statistics (Excoffier *et al.* 2005). The significance of fixation indices was tested using 10 000 permutations.

Present and past distribution modelling

Climatically suitable potential distributions for *Quercus* sect. *Heterobalanus* at the present and during the last glacial maximum (LGM; *ca.* 21 000 before present) were modelled using ENM, which was carried out in MAXENT v3.2 (Phillips *et al.* 2006). Including the distribution records we collected in Table 1, a total of 154 collection records were obtained from the Chinese Virtual Herbarium (http://www.cvh.org.cn/). Numerous herbarium collections from the CVH lack detailed collection records, and the precise GPS locations of specimens from the CVH are only given at the country level, which does not meet the criteria of SDM analyses. Therefore, we only selected the localities with precise records. Meanwhile, some locality data were carefully selected in the analyses. For example, reported localities in Henan and Gansu, as well as some reported localities in Shannxi were not used, because these regions do not contain suitable habitats for the *Quercus* sect. *Heterobalanus*, and the species identifications in these localities were not correct. Thus, we did not consider these unreasonable localities data in the analyses. Based on all records, a climatic niche model was generated using the bioclimatic parameters from the WORLDCLIM database (http://www.worldclim.org) for the current climate and cross the collection localities (Hijmans *et al.* 2005) at a 2.5-arc-min resolution that was used the same method in oak species as Gugger *et al.* (2013). The accuracy of each model prediction was tested by calculating the area under the receiver operating characteristic (ROC) curve (AUC; Fawcett 2006). The restricted bioclimatic data set avoided highly correlated variables and thus prevented potential overfitting (Peterson & Nakazawa 2008). This model was then projected onto the paleoclimatic data set simulated by the COMMUNITY CLIMATE SYSTEM MODEL v3.0 (CCSM3; http://pmip2.lsce.ipsl.fr/) to infer the extent of suitable habitat during the LGM (Collins *et al.* 2006).

Divergence time of cpDNA lineages

Bayesian inferences of divergence times among cpDNA haplotype lineages were estimated using BEAST v1.7.5 (Drummond & Rambaut 2007). Bayesian searches for tree topologies and node ages of the cpDNA data set were conducted in BEAST using a GTR + G substitution model selected by JMODELTEST (Posada 2008) and an uncorrelated lognormal relaxed clock (Dupanloup *et al.* 2002). A Yule process was specified as the tree prior. Ten million generations of the MCMC chains were run, with sampling every 1000th generation after discarding the first 1000 trees as burn-in, and the samples were summarized in the maximum clade credibility tree using TREEANNOTATOR v1.4.8 (Drummond & Rambaut 2007), with the posterior probability limit set to 0.5, and summarizing mean node heights. Final trees were evaluated and edited in FIGTREE v1.3.1. Statistical support for the clades was determined by assessing Bayesian posterior probabilities. Substitution rates and the 95% highest posterior densities (HPDs) were determined with Tracer in combined runs. Divergence times are given as the mean and the 95% HPDs in millions of years, and the 95% HPDs intervals define the precision of estimation. *Fagus*, *Trigonobalanus*, *Cyclobalanopsis* and the other evergreen *Quercus* species were selected as outgroup in accord with previous molecular studies (Manos *et al.* 1999, 2001; Du *et al.* 2016). In the divergence time estimation, the accurate, oldest known fossil of *Quercus* sect. *Heterobalanus* from the middle Miocene Namulin Flora in Tibet (Li & Guo 1976), with an age of 15.10 ± 0.49 Ma, as inferred by ^{40}Ar-^{39}Ar dating (Spicer *et al.* 2003), was used to calibrate the divergence time of this section from other *Quercus* species. The oldest-known *Quercus* fossil, *Q. paleocarpa*, is a fruit fossil reported from Clarno Nut Beds, OR, USA; with an age of 43.8 Ma inferred by ^{40}Ar-^{39}Ar dating (Manchester 1994). *Quercus* includes sub. *Quercus* and sub. *Cyclobalanopsis*. Hence, *Q. paleocarpa* was used to calibrate the divergence time of *Quercus* from other sister linages of Fagaceae. Additionally, *Fagus* has rich fossil records of cupules, nuts, leaves and pollens. The oldest-known *Fagus* fossil, *F. langevinii* (Manchester and Dillhoff 2004), with an age of 47.0–53.0 Ma inferred by K-Ar dating (Ewing 1981), was used to constrain the stem age of the phylogenetic tree.

Ancestral area reconstructions

To undertake ancestral area reconstruction, a Bayesian binary MCMC (BBM) analysis was implemented in RASP v3.0 (RASP, Reconstruct Ancestral State in Phylogenies; http://mnh.scu.edu.cn/soft/blog/RASP) (Yu *et al.* 2015). A total of 10 001 trees produced from the BEAST analysis described above were used. Floristic divisions are generally based on the floral composition and vegetation types across regions (Wu & Wu 1998), as well as the collection sites in the southern Himalayas. The geographic regions that comprise the current flora distributions were defined according to the floristic divisions of China: (A), Sino-Japanese; (B), Sino-Himalayan; (C), South of Himalaya-Nepal; and (D), Malaysia. The number of maximum areas occupied at each node was set to four. To account for phylogenetic uncertainty, ten million generations of the MCMC chains were run, with sampling every 1000th generation. For BBM analyses, 5000 out of 20 000 post-burn-in trees from BEAST were randomly chosen.

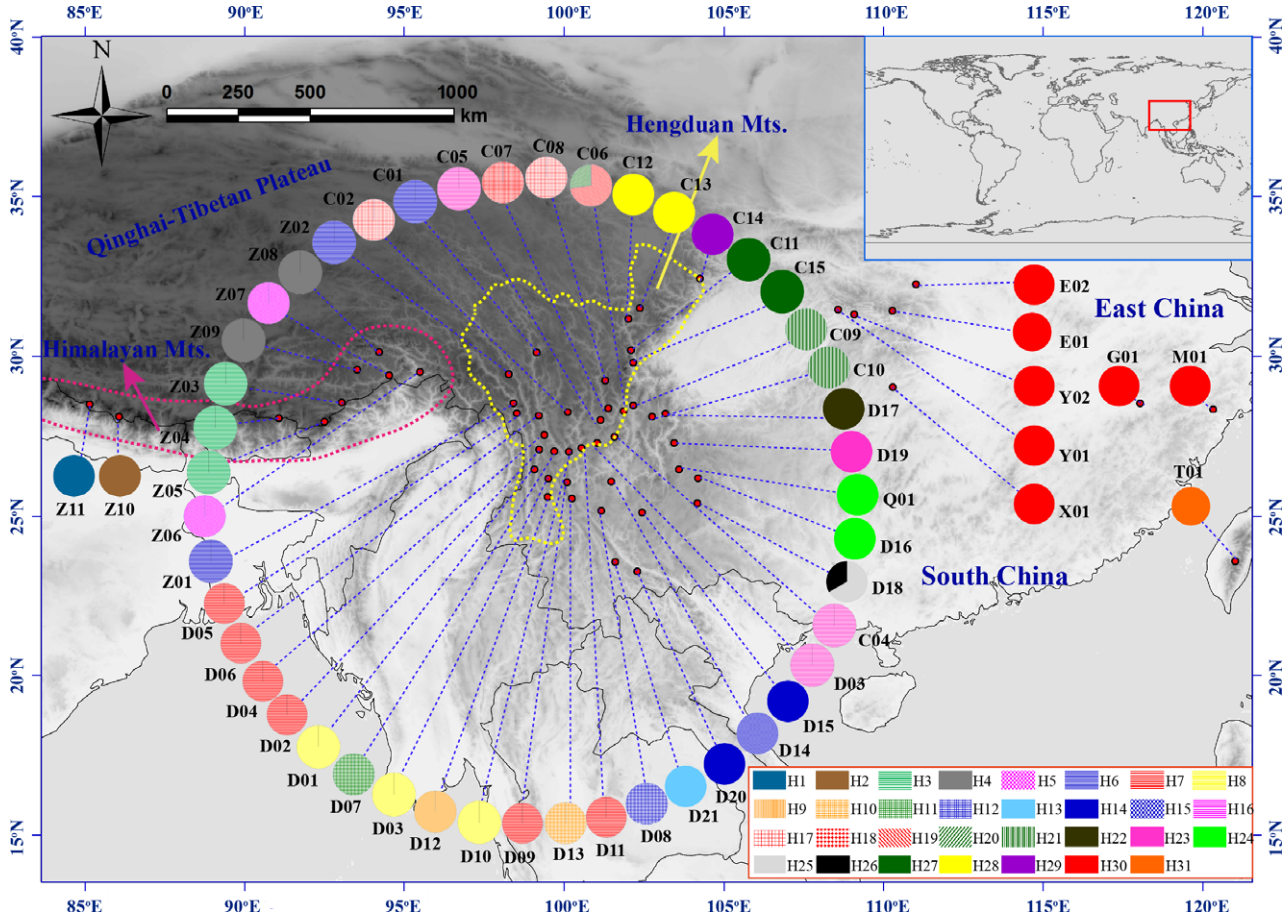

Fig. 2 Geographic distribution of 31 cpDNA haplotypes recovered from 56 *Quercus* sect. *Heterobalanus* populations. The pie charts reflect the frequency of haplotype occurrence in each population. Haplotype colours correspond to those shown in the panel.

Results

Population structure of cpDNA and nSSR diversity

From the sequences of all individuals of *Quercus* sect. *Heterobalanus* in the HHM and surrounding regions, the concatenated cpDNA comprises 3437 base pairs. A total of 31 haplotypes were identified from all plants sampled across the 56 populations (Table 1 and Fig. 2). The basic genetic data for all species in the major regions are summarized in Table 2. At the species level, the cpDNA data revealed high haplotype diversity (H_d = 0.942) and nucleotide diversity (π = 0.005). There was little within-population haplotype variation, as just two populations contained two haplotypes, D18 and C06 (Fig. 2). The other populations were fixed for a single haplotype, and some common haplotypes were shared among different populations, for example H7 and H30 (Fig. 2). In the analysis of differentiation among populations based on cpDNA variation, HAPLONST estimated within-population gene diversity (h_S) as 0.017 (SE 0.012) and total gene diversity (h_T) as 0.963 (SE 0.010). Total cpDNA haplotype diversity (h_T) was higher than average within-population diversity (h_S), which is consistent with the generally very high inter-population differentiation observed (G_{ST} = 0.982). Signatures of phylogeographic structure (i.e. $N_{ST} > G_{ST}$) among populations were also detected (N_{ST} = 0.996, G_{ST} = 0.982; $P < 0.05$). Additionally, significant phylogeographic structure was found at the range-wide scale as determined by PERMUT (N_{ST} = 0.856, G_{ST} = 0.839, $P < 0.05$).

The parsimony network grouped the 31 cpDNA haplotypes into two major clades, Clade A and Clade B (Fig. S1, Supporting information). Clade A included the haplotypes from the southern Himalayas, the lowlands of East China and some adjacent areas of the Hengduan Mountains; Clade B included the haplotypes from highland populations in the Himalayas, the Hengduan Mountains. Spatial genetic analyses of cpDNA haplotypes using SAMOVA indicated that F_{CT} increased to a maximal value of 0.919 when the number of population groups was two (K = 2). Thus, the division by SAMOVA of the chlorotypes from the 56 sampled populations into

Table 2 Molecular diversity indices, neutral tests and demographic estimates from two major regions and all regions of *Quercus* sect. *Heterobalanus*

Group	N*	h†	H_d‡	π§	Tajima's D (P)	Fu's F_S (P)	θ_0¶	θ_1**	τ††	SSD‡‡
Warm	203	14	0.889	0.003	2.2154 ($P < 0.05$)	7.725 ($P < 0.01$)	0.00182	13 571	4.346	0.01786
Cold	326	17	0.915	0.003	1.8398 ($P < 0.05$)	5.256 ($P < 0.01$)	0.07101	13 361	3.272	0.04705
All	529	31	0.952	0.005	2.9608 ($P < 0.01$)	2.409 ($P < 0.02$)	0.08269	18 725	8.170	0.05055

*Sample size (N).
†Number of haplotypes (h).
‡Haplotype diversity (H_d).
§Nucleotide diversity (π).
¶Pre-expansion population size (θ_0).
**Postexpansion population size (Θ_1).
††Time in number of generations, elapsed since the sudden expansion episode (τ).
‡‡The sum of squared differences (SSD).

Table 3 The analysis of molecular variance (AMOVA) for cpDNA data and nSSR data among two geographic regions (Himalaya–Hengduan Mts.; southwest, South/East China) and all populations of *Quercus* sect. *Heterobalanus*

	cpDNA					nSSRs				
Source of variation	d.f.	Sum of squares	Variance components	Percentage of variation (%)	Φ-Statistics	d.f.	Sum of squares	Variance components	Percentage of variation (%)	R-Statistics
Two geographic regions										
Among regions	1	14 606.415	58.31652	91.96	$\Phi_{CT} = 0.91$	1	242.398	0.85759	20.58	$R_{CT} = 0.21$
Among populations with regions	54	2581.261	5.08868	8.02	$\Phi_{SC} = 0.08$	54	667.205	1.02731	24.65	$R_{SC} = 0.25$
With populations	471	3.515	0.00746	0.01	$\Phi_{ST} = 0.01$	494	1127.333	2.28205	54.77	$R_{ST} = 0.54$
Total population										
Among populations	55	17 181.676	53.22748	91.68	$\Phi_{ST} = 0.92$	55	908.603	3.36695	47.18	$R_{ST} = 0.47$
Within populations	471	3.515	0.00746	8.32		494	1127.333	2.28205	52.82	

two groups (regions) is appropriate: (i) populations belonging to the Himalayas and Hengduan Mountains, that is, the cold highlands in high elevation of HHM and (ii) populations belonging to the warm lowlands next to the Hengduan Mountains, East China and the valleys of southern Himalayas. The nonhierarchical AMOVA (Table 3) revealed strong population structure at the species level ($\Phi_{ST} = 0.917$, $P < 0.001$). However, the hierarchical AMOVA showed that 91.96% of the total variation in cpDNA was distributed between the two regions (according to the results of SAMOVA), with 8.12% explained by variation among populations within regions (Table 3).

nSSR-derived AMOVA identified significant, range-wide population genetic differentiation ($R_{ST} = 0.54$, $P < 0.001$), with 20.58% of the variation partitioned between the two regions and 24.65% of the genetic variation occurring among populations within regions (Table 3). In the Bayesian analysis of population structure (Fig. S2, Supporting information), the highest likelihood of the nSSR data was obtained when samples were clustered into two major groups (i.e. $K = 2$). The geographic distribution of nSSR (Fig. 3) was highly congruent with that of cpDNA haplotypes (Fig. S1, Supporting information). According to the assignment plot (Fig. S2c, Supporting information), there are some populations (e.g. D21, Q01, C12 and D08) that showed signs of genetic admixture (see Fig. 3).

Demographic history and ecological niche modelling

Estimates of Tajima's D and Fu's F_S were generally significant for all cpDNA clades and subclades of *Quercus* sect. *Heterobalanus* (Table 2). The observed mismatch

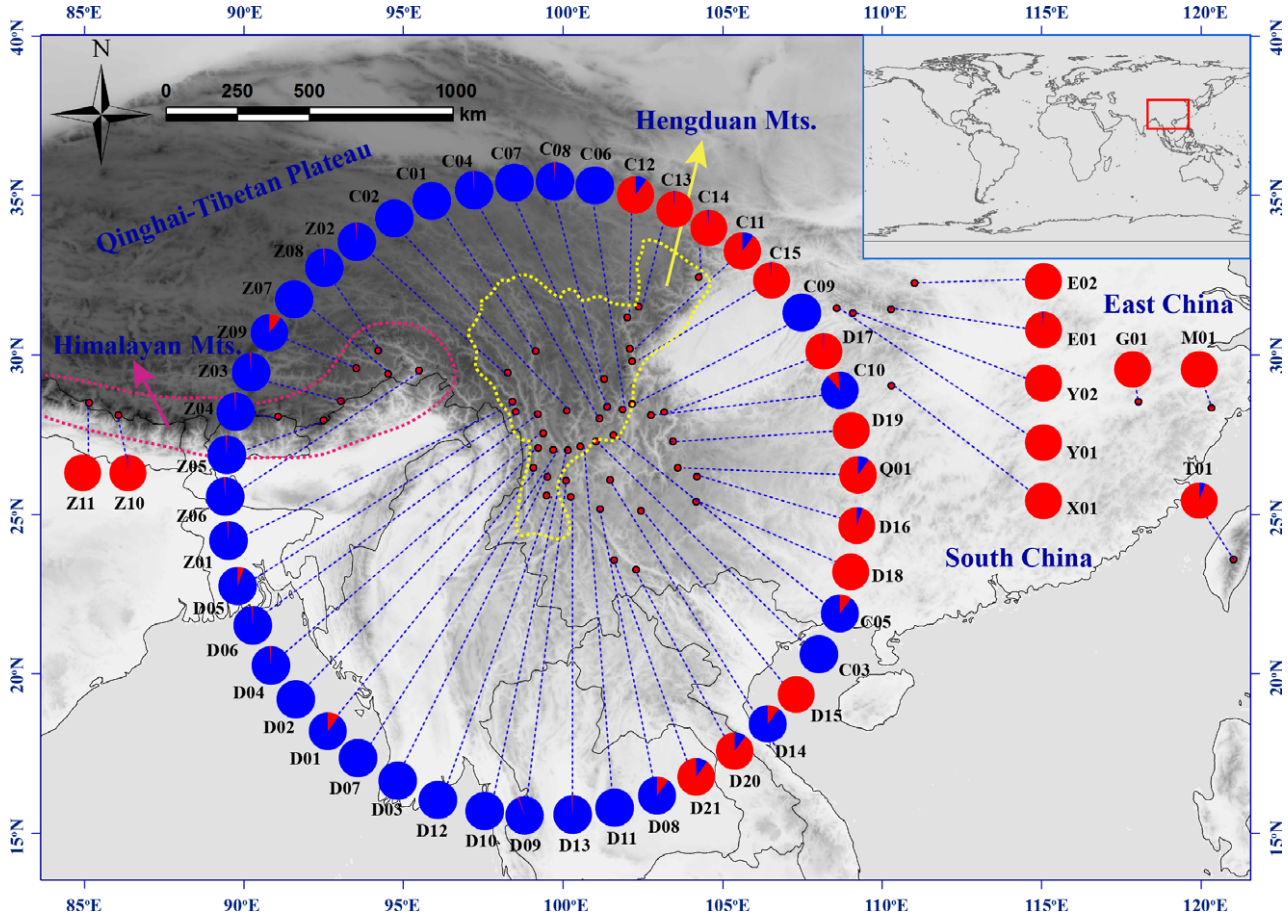

Fig. 3 Geographic distribution of the 56 *Quercus* sect. *Heterobalanus* populations and their colour-coded grouping according to the STRUCTURE analysis.

distributions of cpDNA for each clade/subclade were multimodal and/or very ragged (Fig. S3, Supporting information), and the spatial expansion model was rejected in most cases. The multimodal and ragged distribution shapes generally indicate that populations are stable, not shrinking, or expanded.

For the oaks and climate scenario (the present and the LGM), the area under the receiver operating characteristic curve (AUC) value for the current potential climatically suitable areas of *Quercus* sect. *Heterobalanus* was high (>0.95), indicating good performance of the predictive model. The predicted species distribution under current conditions (1950–2000) was generally similar to the actual species distribution (Fig. 4a), although there were subtle changes in the distribution densities in East China. For the LGM (*ca.* 21 000 yr BP), the northern part of its potential species range was slightly contracted, that is the northern Hengduan Mountains; however, there was a slight expansion in the Himalayas and the eastern parts of the Hengduan Mountains (Fig. 4b).

Divergence time estimation

Estimation of divergence times was carried out in BEAST on the basis of ESS values exceeding 200 across all the nodes discussed as follows. The BEAST-derived cpDNA (*psb*A–*trn*H, *trn*S–*trn*G, *rps*16 and *rpl*32–*trn*L) chronogram of *Quercus* sect. *Heterobalanus* (Fig. 5) recovered 31 haplotypes in six subclades. The age estimates suggested that *Quercus* sect. *Heterobalanus* diverged from their sister lineage of *Quercus ca.* 13.2 Ma (Fig. 5a). Detailed information concerning the divergence of each subclade is summarized in Fig. 5a. The estimated divergence time for the main nodes between the warm region (lineages A-1, A-2, A-3 and A-4) and the cold region (lineages B-1 and B-2) was *ca.* 9.3 Ma. The divergence time of the haplotype from Taiwan, H31, was *ca.* 2.9 Ma.

Ancestral area reconstructions

Based on the topology of the chronogram (Fig. 5), the BBM analysis of ancestral distribution areas (Fig. 6)

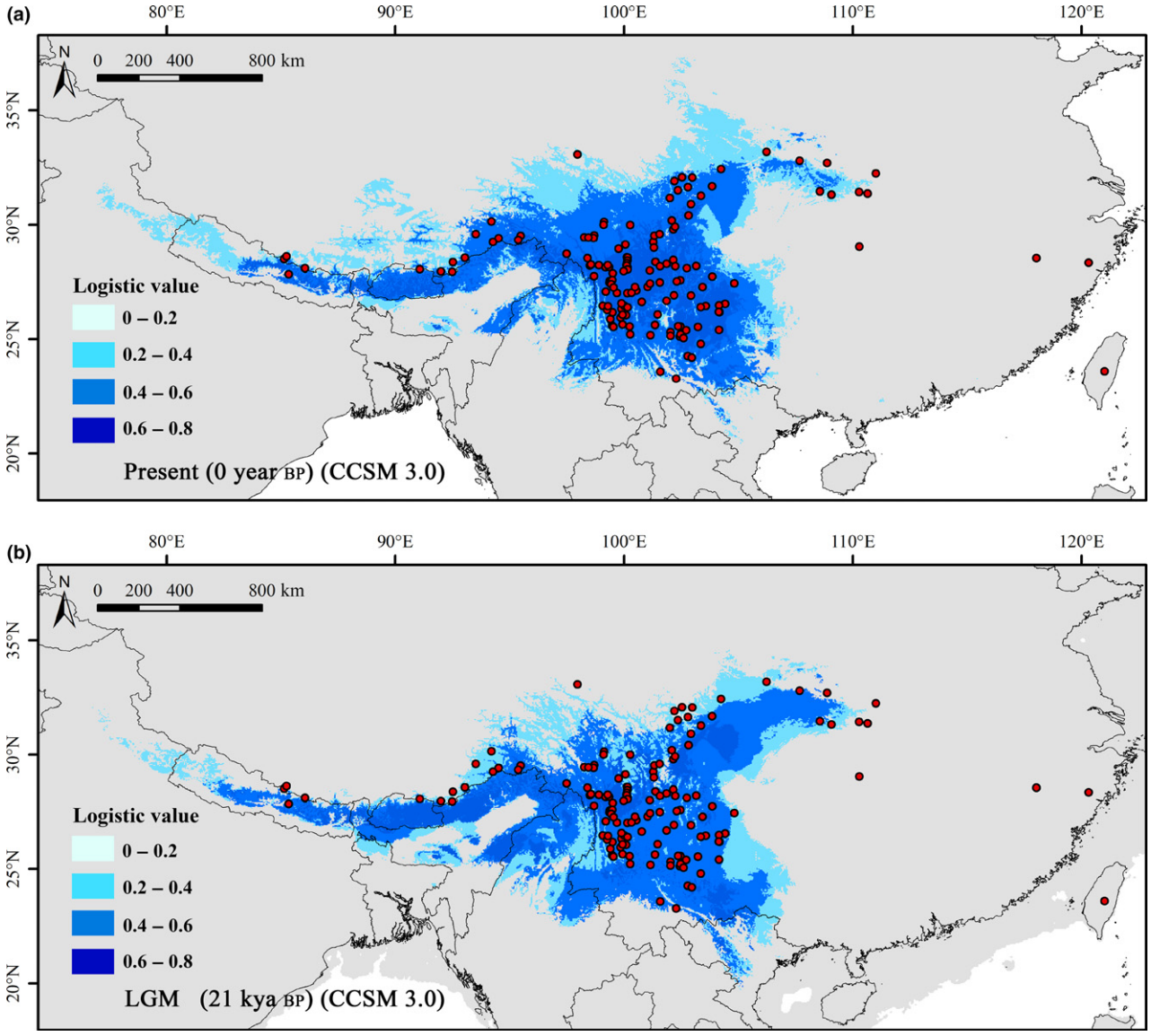

Fig. 4 Potential distributions as probability of occurrence for *Quercus* sect. *Heterobalanus*. (a) under current conditions (1950–2000) and (b) at the last glacial maximum (LGM; 21 000 yr before present; BP). Ecological niche models were established with current bioclimatic variables on the basis of extant occurrence points (red dots) of the species using MAXENT.

supported an ancient distribution of *Quercus* sect. *Heterobalanus* in southwest and East China. Colonization from the warm lowlands (i.e. the low elevation areas adjacent to the eastern Hengduan Mountains, East China, and the deep valleys in southern Himalayas) to cold highlands (i.e. the high elevation of HHM) was inferred. A vicariance event, inferred from evidence of H31, was likely followed by independent dispersal from East China to Taiwan. Taken together with the divergence time of the haplotypes, this illustrates that *Quercus* sect. *Heterobalanus* possibly dispersed from the mainland to Taiwan during the late Pliocene to early Pleistocene (Fig. 5).

Discussion

Haplotype diversity and island-like population genetic structure

In this study, remarkably high levels of genetic diversity were observed among the cpDNA sequences of *Quercus* sect. *Heterobalanus* from the HHM and neighbouring region. The significant differentiation among regions, but high homogeneity within and among populations, indicates significant genetic divergence and a highly structured phylogeographic signal for populations and species of *Quercus* sect. *Heterobalanus*

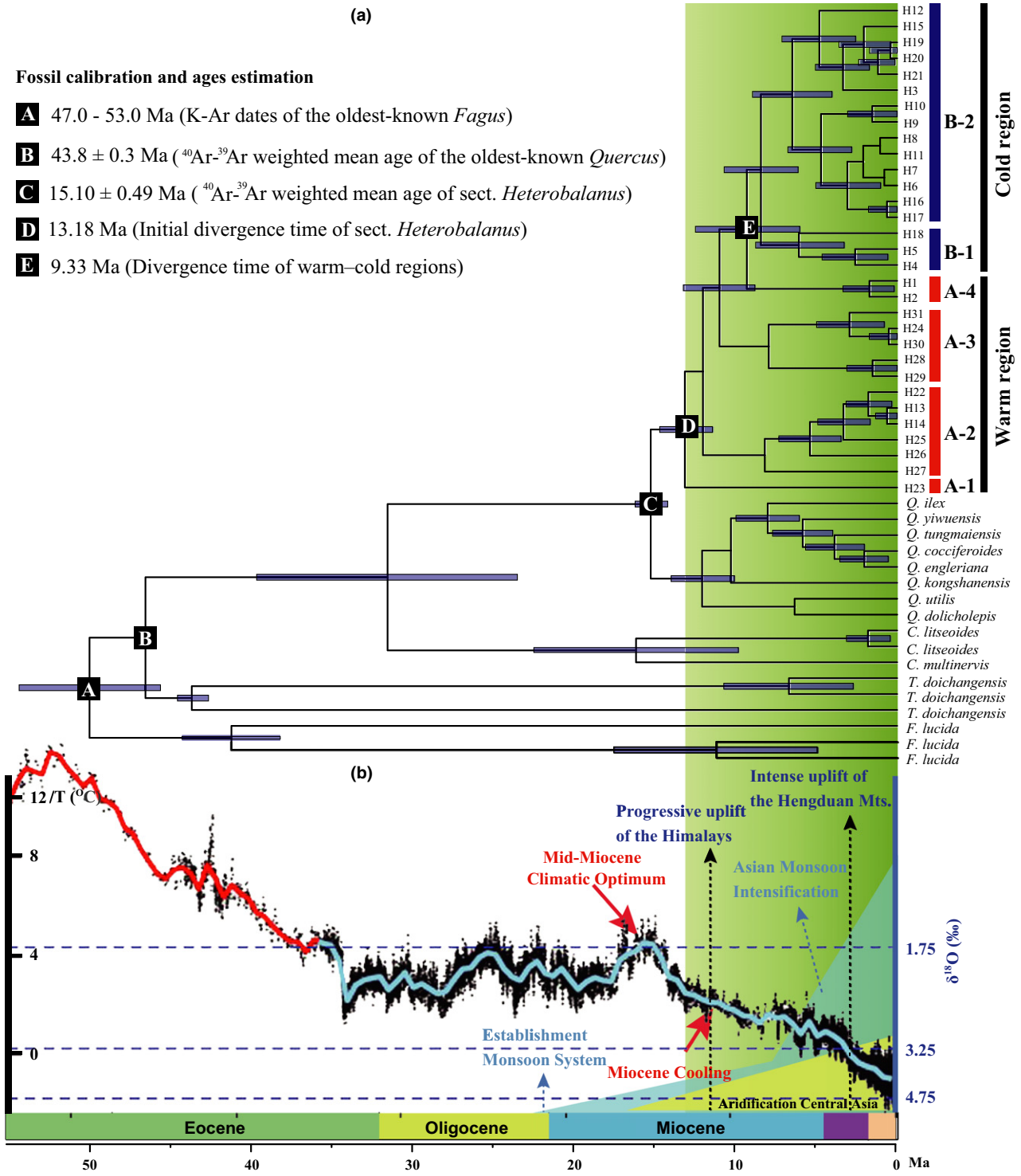

Fig. 5 Estimate of divergence times and the climate and geology in the region of the Himalaya–Hengduan Mountains (HHM). (a) Bayesian divergence time estimates of *Quercus* sect. *Heterobalanus* based on the combined cpDNA sequence data from four cpDNA. The blue bars on the nodes indicate 95% posterior credibility intervals. (b) The climatic and geological events are from Favre *et al.* (2015). Climatic sequence of events including a global average $\delta^{18}O$ curve (right-hand axis) derived from benthic foraminifera which mirrors the major global temperature trends from the Paleocene to Pleistocene (from Zachos *et al.* 2008; Hansen *et al.* 2013); geological sequence of events related to the uplift of the HHM including a graphical representation of the extent of the uplift through time (from Mulch & Chamberlain 2006).

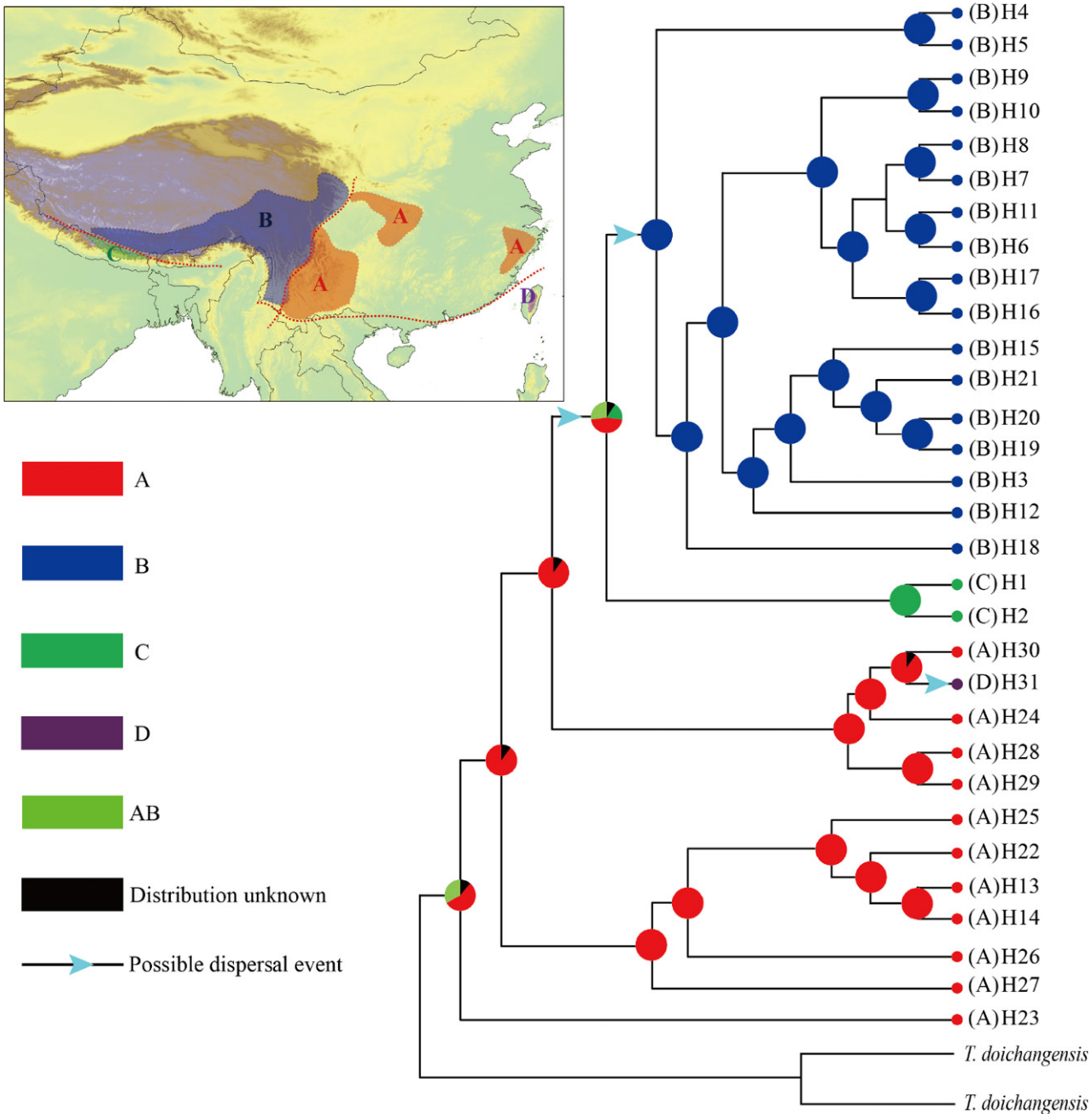

Fig. 6 Ancestral area reconstructions based on the Bayesian binary Markov chain Monte Carlo (BBM) method implemented in RASP using the BEAST-derived chronogram of *Quercus* sect. *Heterobalanus* (Fig. 5). The insert map shows major floristic divisions (A–D) in China according to Wu & Wu (1998). (A), Sino-Japanese; (B), Sino-Himalayan; (C), South of Himalaya-Nepal; (D), Malaysia. Pie charts of each node illustrate the marginal probabilities for each alternative ancestral area derived from BBM with the maximum area number set to four. The colour key identifies possible ancestral ranges at different nodes. Possible dispersal events are indicated by blue arrows.

(Table 3). *Quercus* sect. *Heterobalanus* are distributed in areas of high altitude (Fig. 1h); they are often restricted to high elevations between 2500 m and 4300 m in the HHM, which has likely been the cause of population isolation in different mountain ranges. Warm lowland habitats are restricted to mountain summits at low elevation, especially in East China (e.g. there are three individuals of *Quercus* sect. *Heterobalanus* at the summit of the Sanqing Mountains, Jiangxi; and two oak individuals in Xianju, Zhejiang observed during our field investigation, see Table 1), where are always the evergreen broadleaved forest and the oaks at mountain summits are mixed. Mountains have a direct impact on biodiversity, acting as barriers to some organisms and

bridges for others (Hoorn *et al.* 2013). As the uplift of the HHM caused the surrounding mountain chains to grow as barriers (geographic barriers or/and climatic barriers), previously coherent areas and their populations may have been separated, producing 'island-like' distributions of the *Quercus* sect. *Heterobalanus* populations among different mountain ranges. The oaks might have gone extinct in central regions among the mountain tops during a warm phase of climate oscillation. In that, all these mountain top populations might now occur around the HHM because high elevation gradients served as 'refugia', preventing some populations from going extinct by continuously providing a temporally favourable habitat. Thus, there are no direct genetic connections among the island-like populations, which explains the high diversity among regions, but low diversity within populations (Table 3). Indeed, the SAMOVA identified two well-defined groups corresponding to the divergent cold highlands and warm lowland populations. However, in areas where the cpDNA haplotype frequency varies and genetic barriers are not obvious, the extremely cold environment on the plateau (e.g. the mountain range of the HHM) relative to the lowland must be regarded as a significant climatic barrier, rather than a geographic barrier. Based on the pairwise correlation between genetic and geographic distance measures (Hutchison & Templeton 1999), all species exhibit nonequilibrium population structures. Divergence was largely driven by the effects of genetic drift over time, rather than currently limited gene flow alone.

The genetic structure of *Quercus* sect. *Heterobalanus* is consistent with the fact that its pollen dispersal is limited by thick forest and complex topography, as well as seed dispersal is limited by the inability of transmitters go through the deep valleys and rivers. This can explain their highly fragmented habitats in the 'sky-island system' of the HHM region and the isolated summits of mountains in East China occurred. Moreover, the high level of total genetic diversity and low levels of within-population diversity are typical for high mountainous plants, especially in island-like populations (Luo *et al.* 2016). Previous studies have shown that species restricted to sky islands commonly have high levels of interpopulation genetic divergence (Shepard & Burbrink 2009), consistent with the significant differentiation between these oak populations. Although many sky-island species in other regions show high levels of isolation among mountain clusters, our data indicate that *Quercus* sect. *Heterobalanus* diversification has occurred on a broader geographic scale, spanning cold highland (e.g. HHM) and warm lowland (e.g. East China) regions. These mountain regions may not be equivalent ecologically (especially with respect to temperature), and the *Quercus* sect. *Heterobalanus* occurring cross such wide ranges span different climatic regions may therefore have experienced different selective pressures. Above all, the ecological shift from warm lowland to cold highland environments requires adaption to the climatic conditions. The lineage of *Quercus* has been well documented that the sclerophyllous leaves in response to changing climates are consistent with the adaptive radiations under distinctly summer-dry and winter-dry climates (Bouchal *et al.* 2014). The changing climatic conditions may therefore underlie some of the molecular differentiation and evolution observed among the two population clusters.

Distribution and demographic history

Based on a MDA using cpDNA, each clade (or subclade) exhibited a ragged multimodal distribution (Fig. S3, Supporting information), suggesting that *Quercus* sect. *Heterobalanus* has not experienced recent demographic expansion events. Additionally, we did not detect a geographic region that could reasonably be regarded as a glacial refugium, that is a region with a higher haplotype diversity than elsewhere (Table 1, Fig. 2). This is consistent with the results from the past (LGM) and the present distribution modelling, indicating that the broadscale distributions of *Quercus* sect. *Heterobalanus* remained fairly stable, even during the last glacial/postglacial cycle (Fig. 4). Overall, these results are consistent with some plant taxa in the HHM, such as, *Eriophyton wallichii*, *Thalictrum squamiferum*, *Paraquilegia microphylla* and *Chionocharis hookeri* (Luo *et al.* 2016). This pattern may have been caused by adaptation to the changing environment, and the population equilibrium of *Quercus* sect. *Heterobalanus* in the past and the present is also likely associated with the evolution of multiple epidermis in response to the climatic cooling, ultraviolet (UV) radiation and aridification concomitant with the plateau uplift process (Sun *et al.* 2015; Zhou *et al.* 1994). The special physiological properties, for example, the adaptive plasticity of leaves in response to environmental effects on the plateau (e.g. UV-B irradiation and precipitation) at high elevations (Sun *et al.* 2015); and the high efficiency of photosynthetic nitrogen used at altitudes of 3240–3610 m (Zhang *et al.* 2007), benefited the oaks to go through and survive during the environmental changes. Additionally, glaciation probably did not have a profound influence on *Quercus* sect. *Heterobalanus* in areas, although the HHM has many snowy mountains. The overall stability of populations may be related to the geological event that unified the ice sheets covering the high elevation of the HHM. Because the ice sheets never fully formed and expanded into the plateau glaciers, being less

uniform in the QTP than in other regions of the Northern Hemisphere (Shi *et al.* 1998; Owen *et al.* 2008; Kirchner *et al.* 2011). Glacial climatic conditions were not inherently unfavourable or restrictive for all plant species in areas, so the HHM may not have served as 'refugia' for the oaks. *Quercus* sect. *Heterobalanus*, with a wider range of habitats and vegetation zones were certainly able to survive in the HHM throughout glacial periods. Although the other warm tropical/subtropical plants were restricted by the cold environments associated with the plateau uplifting, *Quercus* sect. *Heterobalanus* colonized these emerging cold highland areas.

These results show that climatic oscillations, especially during the LGM, had minimal effects on distribution ranges, suggesting that *Quercus* sect. *Heterobalanus* adapted to cold environments by gradually colonizing the plateau from warm evergreen broadleaf forests, while other thermophilous plants retreated. They subsequently became the dominant trees as the rising of the HHM.

The HHM uplift, climatic cooling and colonization

The effects of geological and climate dynamics on species diversification have been a central topic of debate for several years; in particular, the uplift of the plateau (e.g. Tibetan plateau, Himalayas, Hengduan Mountains) likely has played an important role in the evolutionary history of organisms (Favre *et al.* 2015). An increasing number of studies have focused on the biology and geology of this region; however, the origin and evolution of diversity hotspots associated with the HHM uplift have remained unclear and controversial for years. Previous studies indicated the QTP experienced expansion during the Miocene and the Pliocene (Li & Fang 1999; Mulch & Chamberlain 2006), particularly at its eastern edge, which encompasses several mountain ranges and includes the HHM biodiversity hotspot. During the QTP uplift, the warmest interval of the Neogene occurred, known as the Middle Miocene Climatic Optimum (MMCO) (Flower & Kennett 1994), which was followed by one of the most prominent climatic cooling events. The East Asian monsoonal system has been interpreted as an environmental response to a major phase of the uplift (An *et al.* 2001). The molecular dating suggests that *Quercus* sect. *Heterobalanus* initially diverged as the climate cooled after the MMCO (Fig. 5). The cpDNA results illustrate that *Quercus* sect. *Heterobalanus* is comprised of six main lineages with haplotypes from the warm and cold regions (Fig. 5a). Additionally, together with paleobotanical evidence, molecular dating (Fig. 5) and ancestral area reconstruction analyses (Fig. 6), the results indicate that *Quercus* sect. *Heterobalanus* grew in the warm broadleaf mixed forests; subsequently, they became the dominant trees in the surrounding mountain ranges with the HHM uplift and relevant climatic cooling. In the northeastern Hengduan Mountains, H23 is the relatively primary lineage from present-day subtropical broadleaf mixed forests, and the H25 and H26 lineages are also from the subtropical region (Fig. 5a). The oldest-known *Quercus* sect. *Heterobalanus* fossils have been reported in the mid-Miocene Namulin flora, where broadleaf plants in this region have been discovered (Li & Guo 1976). However, present-day Namulin has no broadleaf plants, indicating the transformation from warm temperate flora to the cold plateau flora. Mid-Miocene *Quercus* sect. *Heterobalanus* have also been reported in the Xiaolongtan flora where included typical subtropical vegetation, such as Leguminosae, Fagaceae, Lauraceae and Magnoliaceae (Tao 2000). Thus, the paleobotanical evidence also indicated that *Quercus* sect. *Heterobalanus* originated from tropical or subtropical forests. The common ancestors of the section likely spread into adjacent southwestern China no later than the start of the MMCO (*ca.* 15 Ma). The clades diversified during the progressive uplift of the Himalayas, Asian Monsoon intensification and the Miocene climatic cooling (Fig. 5b), as the global average temperature gradually decreased (Zachos *et al.* 2008; Hansen *et al.* 2013). Miocene fossil records from the Himalayas, and the lineages of the southern Himalayas (i.e. H1 from Jilong and H2 from Zhangmu) clustered with lineages from warm regions, implying that 'warm–cold colonization' of *Quercus* sect. *Heterobalanus* was a response to the HHM uplift. A phylogeographic study of the warm evergreen oaks, *Quercus glauca*, revealed that two major haplotype lineages (southwest China versus southeast China and East China Sea) were separated by the topographic barrier of the Himalayan uplift in the Miocene which allowed the two lineages to diverge (Xu *et al.* 2015), providing evidence that the colonization event was caused by the Himalayan uplift.

The uplift of the HHM altered the climate from warm to cold, which acted as a barrier to distribution and resulted in lineage divergence and speciation in warm and cold regions at approximately 9.3 Ma (Fig. 5a). This resulted in differentiation among *Quercus* sect. *Heterobalanus* from the HHM (cold regions) and peripheral regions in the lowland (warm regions). The continued uplift of the Himalayas limited genetic exchange between populations in the high HHM and other warm lowlands, intensifying in the diversification of taxa in cold regions (lineages B1 and B2) at approximately 8.5 Ma (Fig. 5a). Fossil records suggested that *Quercus* sect. *Heterobalanus* were not the dominant species, but rather were part of mixed evergreen broadleaf forests as companion species in the Miocene (Zhou 1993),

supporting the viewpoint that *Quercus* sect. *Heterobalanus* increased in abundance at high elevation during the HHM uplift and climatic cooling. At that time, a significant climatic shift from a warm subtropical climate to a cold plateau climate during the HHM uplift triggered a split between the warm group and the cold group, based on our ancestral area inference. On the basis of the above-mentioned molecular analyses and paleobotanical evidence, we hypothesize that *Quercus* sect. *Heterobalanus* initially diverged no later than the mid-Miocene and coexisted with species in warm evergreen broadleaf forests, with large ranges in the Miocene. They gradually colonized the plateau and became the dominant trees during the HHM uplift. Thus, the 'warm–cold colonization' hypothesis is proposed to explain the response of *Quercus* sect. *Heterobalanus* to the HHM uplift, specifically stating that the HHM uplift created new habitats and climate regimes for the oaks.

Implications of the geological evolution of the HHM

The highly conserved evolutionary history from the BEAST-based phylogeny of *Quercus* sect. *Heterobalanus* (Fig. 5a) is in accordance with climatic change over geological time (Fig. 5b). This, coupled with present distribution in the cold plateau and other warm regions, makes the oak group an ideal model for examining geological and environmental changes in the HHM since the mid-Miocene.

According to molecular dating, *Quercus* sect. *Heterobalanus* initially diverged during the mid-Miocene, and rapid divergence of the major clades occurred from the mid-Miocene to the Pliocene (Fig. 5a), which suggest the relevant geographic and potential paleoclimatic changes. From the paleobotanical and lithological evidence, the radical changes in climate and vegetation of the QTP occurred from the Oligocene to the Miocene (Quade *et al.* 1989; Rea *et al.* 1998; An *et al.* 2001). *Quercus* sect. *Heterobalanus* co-existed with other species in evergreen broadleaf forests in the Miocene and subsequently became the dominant trees in evergreen sclerophyllous forests since the Pliocene (Zhou 1993; Tao 2000). Although the timing and mechanisms of the HHM uplift and their effects on organisms have been uncertain, our molecular dating is consistent with the previous studies, for example, foliage fossil data, paleobotanical evidence and lithological and sedimentary data (Quade *et al.* 1989; Rea *et al.* 1998; An *et al.* 2001). Thus, our results suggest the geological evolution of the HHM from a biological perspective, that is *Quercus* sect. *Heterobalanus* adapted to the cold environment, colonized the plateau and diverged as the environment changed.

Geological analyses based on magnetostratigraphy, sedimentology, $^{40}Ar/^{39}Ar$ of fission-track studies, and isotope dating of paleosoils suggested that the QTP arose 50 Ma ago, indicating that the central plateau having been relatively high by 35–40 Ma (Lippert *et al.* 2014). Recently, an increasing number of geological studies have made progress and illuminated events underlying the spatiotemporal changes in different parts of the QTP from different approaches; however, the spatiotemporal scale still are debated (Harrison *et al.* 1992; Yin & Harrison 2000; Tapponnier *et al.* 2001; Mulch & Chamberlain 2006; Royden *et al.* 2008; Lippert *et al.* 2014; Favre *et al.* 2015; Li *et al.* 2015). From the present study, we cannot infer detailed information about the initial uplift of the HHM. However, the results demonstrate that the split between populations within the two regions was associated with a major tectonic event along the uplift of the HHM. Therefore, we suggest that the HHM was indeed raised to a certain height after the mid-Miocene, thus caused the genetic discontinuities of *Quercus* sect. *Heterobalanus* between the cold highlands and warm lowlands. The late Miocene uplift event began at *ca.* 8.5 or 9 Ma and involved the Himalayas and possibly some southern portions of the Tibetan plateau (Rea *et al.* 1998). Additionally, the paleoelevation of the QTP suggested that the orogeny of the Hengduan Mountains occurred as a final propagation of the uplift after 10 Ma (Mulch & Chamberlain 2006). The dating of *Quercus* sect. *Heterobalanus* supports the geological hypothesis that a rapid uplift of eastern Tibet took place at approximately 8 Ma (Harrison *et al.* 1992; Molnar *et al.* 1993; An *et al.* 2001). The populations along the surrounding region of the eastern Hengduan Mountains include haplotypes observed in warm regions, for example, H28 and H29 (Figs 2 and 5a), revealing heterozygosity among chloroplast haplotypes in warm and cold ecotones. However, most populations in the plateau clustered as a cold-region lineage (Fig. 5a), which diverged at *ca.* 8.5 Ma, suggesting that the HHM intensely uplifted in the late Miocene to early Pliocene. The results support the geological hypothesis that the Himalayas rose 3000 m since the Pliocene based on the dating of *Quercus semecarpifolia* fossil from the Xixiabangma (Hsu *et al.* 1973). Other studies based on the fossils have also suggested that Namulin and Xixiabangma have risen more than 2000 m since the Pliocene (e.g. Zhou *et al.* 2007). The oaks inhabit altitudes of nearly 1000 m in warm lowlands and up to 4300 m in cold plateau regions (Table 1, Fig. 1). Members of this species group have adapted progressively as the HHM experienced significant increases in altitude to at least the 3000-m level. Alternatively, paleobotanical and paleoclimatic data suggested that the Hengduan Mountains underwent significant uplift after the Miocene, reaching their peak elevation shortly before the late Pliocene (Sun *et al.* 2011), supporting our results.

In short, our data and analyses clarify large-scale features of the HHM history and topography in a framework which is consistent with the evolutionary history of *Quercus* sect. *Heterobalanus*. Molecular dating reveals that the HHM exhibited uplift during the late Miocene to early Pliocene, providing novel insight into the spatiotemporal evolutionary history of the HHM from a biological perspective. The progressive uplift of the Himalayas in the mid-Miocene, intensive uplift of Hengduan Mountains and the Miocene cooling in a global context (Fig. 5b) fit well with our model of oak biogeography. That is, the HHM uplift created new habitats and climate regimes, favouring speciation in some taxa such as *Quercus* sect. *Heterobalanus*. The lowland region of the eastern HHM and the valleys of the plateau continued to harbour older lineages while accommodating more recently diverged lineages from the nearby the HHM. Environmental effects influenced the oaks' geographic distribution pattern, whereas the response of the oaks to the uplift, colonizing from the warm region to cold plateau, which imprinted the geological evolution of the HHM. Therefore, to a certain extent, the evolutionary history of these oaks illuminates the geological uplift of the HHM.

Acknowledgements

We are grateful to the five anonymous reviewers for their constructive comments greatly improved the quality of the manuscript. Also, we would like to thank Raymond Porter for revising English; Robert A. Spicer for the suggestions; Lin-Bo Jia and Min Deng for material collection; Bin Tian, Dong-Rui Jia, Yong-Shuai Sun, Jian-Feng Huang and Xiu-Qin Ci for their kind help with molecular data analyses and experiments. This study was financially supported by the Major Program of National Natural Science Foundation of China (No. 31590820, 31590823) and the National Natural Science Foundation of China (No. U1502231).

References

Aldrich PR, Michler CH, Sun W, Romero-Severson J (2002) Microsatellite markers for northern red oak (Fagaceae: *Quercus rubra*). *Molecular Ecology Notes*, **2**, 472–474.

An ZS, Kutzbach JE, Prell WL, Porter SC (2001) Evolution of Asian monsoons and phased uplift of the Himalaya-Tibetan plateau since Late Miocene times. *Nature*, **411**, 62–66.

Axelrod DI (1975) Evolution and biogeography of Madrean-Tethyan sclerophyll vegetation. *Annals of the Missouri Botanical Garden*, **62**, 280–334.

Bandelt HJ, Forster P, Röhl A (1999) Median-joining networks for inferring intraspecific phylogenies. *Molecular Biology and Evolution*, **16**, 37–48.

Bouchal J, Zetter R, Grímsson F, Denk T (2014) Evolutionary trends and ecological differentiation in early Cenozoic Fagaceae of western North America. *American Journal of Botany*, **101**, 1332–1349.

Che J, Zhou WW, Hu JS *et al.* (2010) Spiny frogs (*Paini*) illuminate the history of the Himalayan region and Southeast Asia. *Proceedings of the National Academy of Sciences of the United States of America*, **107**, 13765–13770.

Collins WD, Bitz CM, Blackmon ML (2006) The community climate system model version 3 (CCSM3). *Journal of Climate*, **19**, 2122–2143.

Coombs J, Letcher B, Nislow K (2008) CREATE: a software to create input files from diploid genotypic data for 52 genetic software programs. *Molecular Ecology Resources*, **8**, 578–580.

Ding L, Spicer R, Yang J *et al.* (2017) Quantifying the rise of the Himalaya orogen and implications for the South Asian monsoon. *Geology*, **45**, 215–218.

Dow B, Ashley M, Howe H (1995) Characterization of highly variable (GA/CT) n microsatellites in the bur oak, *Quercus macrocarpa*. *Theoretical and Applied Genetics*, **91**, 137–141.

Drummond AJ, Rambaut A (2007) BEAST: Bayesian evolutionary analysis by sampling trees. *BMC Evolutionary Biology*, **7**, 214.

Du FK, Hou M, Wang W, Mao K, Hampe A (2016) Phylogeography of *Quercus aquifolioides* provides novel insights into the Neogene history of a major global hotspot of plant diversity in south-west China. *Journal of Biogeography*, **44**, 294–307.

Dupanloup I, Schneider S, Excoffier L (2002) A simulated annealing approach to define the genetic structure of populations. *Molecular Ecology*, **11**, 2571–2581.

Evanno G, Regnaut S, Goudet J (2005) Detecting the number of clusters of individuals using the software STRUCTURE: a simulation study. *Molecular Ecology*, **14**, 2611–2620.

Ewing TE (1981) Regional stratigraphy and structural setting of the Kamloops Group, south-central British Columbia. *Canadian Journal of Earth Science*, **18**, 1464–1477.

Excoffier L, Laval G, Schneider S (2005) Arlequin (version 3.0): an integrated software package for population genetics data analysis. *Evolutionary Bioinformatics* Online, **1**, 47.

Falush D, Stephens M, Pritchard JK (2003) Inference of population structure using multilocus genotype data: linked loci and correlated allele frequencies. *Genetics*, **164**, 1567–1587.

Favre A, Päckert M, Pauls SU *et al.* (2015) The role of the uplift of the Qinghai-Tibetan Plateau for the evolution of Tibetan biotas. *Biological Reviews*, **90**, 236–253.

Fawcett T (2006) An introduction to ROC analysis. *Pattern Recognition Letters*, **27**, 861–874.

Fazekas AJ, Steeves R, Newmaster SG (2010) Improving sequencing quality from PCR products containing long mononucleotide repeats. *BioTechniques*, **48**, 277–285.

Flower BP, Kennett JP (1994) The middle Miocene climatic transition: East Antarctic ice sheet development, deep ocean circulation and global carbon cycling. *Palaeogeography, Palaeoclimatology, Palaeoecology*, **108**, 537–555.

Fu YX (1997) Statistical tests of neutrality of mutations against population growth, hitchhiking and background selection. *Genetics*, **147**, 915–925.

George AD, Marshallsea SJ, Wyrwoll KH, Chen J, Lu YC (2001) Miocene cooling in the northern Qilian Shan, northeastern margin of the Tibetan Plateau, revealed by apatite fission-track and vitrinite-reflectance analysis. *Geology*, **29**, 939–942.

Gugger PF, Ikegami M, Sork VL (2013) Influence of late Quaternary climate change on present patterns of genetic variation in valley oak, Quercus lobata Nee. *Molecular Ecology*, **22**, 3598–3612.

Hamilton M (1999) Four primer pairs for the amplification of chloroplast intergenic regions with intraspecific variation. *Molecular Ecology*, **17**, 513–525.

Hansen J, Sato M, Russell G, Kharecha P (2013) Climate sensitivity, sea level and atmospheric carbon dioxide. *Philosophical Transactions of the Royal Society of London A: Mathematical, Physical and Engineering Sciences*, **371**, 20120294.

Harpending H (1994) Signature of ancient population growth in a low-resolution mitochondrial DNA mismatch distribution. *Human Biology*, **66**, 591–600.

Harrison TM, Copeland P, Kidd W, Yin A (1992) Raising tibet. *Science*, **255**, 1663–1670.

He YL, Li N, Wang ZX (2014) *Quercus yangyiensis* sp. nov. from the Late Pliocene of Baoshan, Yunnan and its Paleoclimatic significance. *Acta Geologica Sinica (English Edition)*, **88**, 738–747.

Hijmans RJ, Cameron SE, Parra JL, Jones PG, Jarvis A (2005) Very high resolution interpolated climate surfaces for global land areas. *International Journal of Climatology*, **25**, 1965–1978.

Hoorn C, Mosbrugger V, Mulch A, Antonelli A (2013) Biodiversity from mountain building. *Nature Geoscience*, **6**, 154.

Hsu J, Tao JR, Sun XJ (1973) On the discovery of a *Quercus semicarpifolia* bed at Mount Shisha Pangma and its significance in botany and geology. *Acta Botanica Sinica*, **15**, 103–119.

Huang CJ, Zhang YT, Bartholomew B (1999) Fagaceae. In: *Flora of China* (eds Wu ZY, Raven PH), pp. 314–400. Science Press, Missouri Botanical Garden,, Beijing, St Louis, Missouri.

Huang HS, Hu JJ, Su T, Zhou ZK (2016) The occurrence of *Quercus heqingensis* n. sp. and its application to palaeo-CO_2 estimates. *Chinese Science Bulletin*, **12**, 1354–1364.

Hubisz MJ, Falush D, Stephens M, Pritchard JK (2009) Inferring weak population structure with the assistance of sample group information. *Molecular Ecology Resources*, **9**, 1322–1332.

Hutchison DW, Templeton AR (1999) Correlation of pairwise genetic and geographic distance measures: inferring the relative influences of gene flow and drift on the distribution of genetic variability. *Evolution*, **53**, 1898–1914.

Jia DR, Abbott RJ, Liu TL, Mao KS, Bartish IV, Liu JQ (2012) Out of the Qinghai-Tibet Plateau: evidence for the origin and dispersal of Eurasian temperate plants from a phylogeographic study of *Hippophae rhamnoides* (Elaeagnaceae). *New Phytologist*, **194**, 1123–1133.

Kampfer S, Lexer C, Glössl J, Steinkellner H (1998) Characterization of (GA)n microsatellite loci from *Quercus robur*. *Hereditas*, **129**, 183–186.

Kirchner N, Greve R, Stroeven AP, Heyman J (2011) Paleoglaciological reconstructions for the Tibetan Plateau during the last glacial cycle: evaluating numerical ice sheet simulations driven by GCM-ensembles. *Quaternary Science Reviews*, **30**, 248–267.

Li JJ, Fang XM (1999) Uplift of the Tibetan Plateau and environmental changes. *Chinese Science Bulletin*, **44**, 2117–2124.

Li HM, Guo SX (1976) Miocene flora of Nanmulin in Tibet. *Acta Palaeontologica Sinca*, **15**, 7–17.

Li L, Abbott RJ, Liu B *et al.* (2013) Pliocene intraspecific divergence and Plio-Pleistocene range expansions within *Picea likiangensis* (Lijiang spruce), a dominant forest tree of the Qinghai-Tibet Plateau. *Molecular Ecology*, **22**, 5237–5255.

Li JJ, Zhou SZ, Zhao ZJ, Zhang J (2015) The Qingzang movement: the major uplift of the Qinghai-Tibetan Plateau. *Science China Earth Sciences*, **58**, 2113–2122.

Librado P, Rozas J (2009) DnaSP v5: a software for comprehensive analysis of DNA polymorphism data. *Bioinformatics*, **25**, 1451–1452.

Lippert PC, van Hinsbergen DJJ, Dupont-Nivet G (2014) Early Cretaceous to present latitude of the central proto- Tibetan Plateau: a paleomagnetic synthesis with implications for Cenozoic tectonics, paleogeography, and climate of Asia. In: *Toward an improved understanding of uplift mechanisms and the elevation history of the Tibetan Plateau* (eds Nie J, Horton BK, Hoke GD). *Geological Society of America Special Paper*, **507**, 1–21.

Liu JQ, Duan YW, Hao G, Ge XJ, Sun H (2014) Evolutionary history and underlying adaptation of alpine plants on the Qinghai-Tibet Plateau. *Journal of Systematics and Evolution*, **52**, 241–249.

Luo D, Yue JP, Sun WG *et al.* (2016) Evolutionary history of the subnival flora of the Himalaya-Hengduan Mountains: first insights from comparative phylogeography of four perennial herbs. *Journal of Biogeography*, **43**, 31–43.

Manchester SR (1994) Fruits and seeds of the Middle Eocene Nut Beds Flora, Clarno Formation, Oregon. *Palaeontographic Americana*, **58**, 1–205.

Manchester SR, Dillhoff RM (2004) *Fagus* (Fagaceae) fruits, foliage, and pollen from the middle Eocene of Pacific Northwestern North America. *Canadian Journal of Botany*, **82**, 1509–1517.

Manos PS, Doyle JJ, Nixon KC (1999) Phylogeny, biogeography, and processes of molecular differentiation in *Quercus* subgenus *Quercus* (Fagaceae). *Molecular Phylogenetics and Evolution*, **12**, 333–349.

Manos PS, Zhou ZK, Cannon CH (2001) Systematics of Fagaceae: phylogenetic tests of reproductive trait evolution. *International Journal of Plant Sciences*, **162**, 1361–1379.

Meng HH, Zhang ML (2011) Phylogeography of *Lagochilus ilicifolius* (Lamiaceae) in relation to quaternary climatic oscillation and aridification in northern China. *Biochemical Systematics and Ecology*, **39**, 787–796.

Meng HH, Zhang ML (2013) Diversification of plant species in arid Northwest China: species-level phylogeographical history of *Lagochilus* Bunge ex Bentham (Lamiaceae). *Molecular Phylogenetics and Evolution*, **68**, 398–409.

Meng HH, Jacques MBF, Su T *et al.* (2014) New biogeographic insight into *Bauhinia* s.l. (Leguminosae): Integration from fossil records and molecular analyses. *BMC Evolutionary Biology*, **14**, 181.

Molnar P, England P, Martinod J (1993) Mantle dynamics, uplift of the Tibetan Plateau, and the Indian monsoon. *Reviews of Geophysics*, **31**, 357–396.

Mulch A, Chamberlain CP (2006) Earth science: the rise and growth of Tibet. *Nature*, **439**, 670–671.

Myers N, Mittermeier RA, Mittermeier CG, Da Fonseca GA, Kent J (2000) Biodiversity hotspots for conservation priorities. *Nature*, **403**, 853–858.

Owen LA, Caffee MW, Finkel RC, Seong YB (2008) Quaternary glaciation of the Himalayan-Tibetan orogen. *Journal of Quaternary Science*, **23**, 513–531.

Oxelman B, Lidén M, Berglund D (1997) Chloroplast *rps*16 intron phylogeny of the tribe Sileneae (Caryophyllaceae). *Plant Systematics and Evolution*, **206**, 393–410.

Peterson A, Nakazawa Y (2008) Environmental data sets matter in ecological niche modelling: an example with *Solenopsis invicta* and *Solenopsis richteri*. *Global Ecology and Biogeography*, **17**, 135–144.

Phillips SJ, Anderson RP, Schapire RE (2006) Maximum entropy modeling of species geographic distributions. *Ecological Modelling*, **190**, 231–259.

Pons O, Petit R (1996) Measwring and testing genetic differentiation with ordered versus unordered alleles. *Genetics*, **144**, 1237–1245.

Posada D (2008) jModelTest: phylogenetic model averaging. *Molecular Biology and Evolution*, **25**, 1253–1256.

Pritchard JK, Wen W, Falush D (2003). Documentation for structure software: version 2.3. http://pritch.bsd.uchicago.edu/structure.htm.

Qiu YX, Fu CX, Comes HP (2011) Plant molecular phylogeography in China and adjacent regions: tracing the genetic imprints of Quaternary climate and environmental change in the world's most diverse temperate flora. *Molecular Phylogenetics and Evolution*, **59**, 225–244.

Quade J, Cerling TE, Bowman JR (1989) Development of Asian monsoon revealed by marked ecological shift during the latest Miocene in northern Pakistan. *Nature*, **342**, 163–166.

Rea DK, Snoeckx H, Joseph LH (1998) Late Cenozoic eolian deposition in the North Pacific: Asian drying, Tibetan uplift, and cooling of the northern hemisphere. *Paleoceanography*, **13**, 215–224.

Renner SS (2016) Available data point to a 4-km-high Tibetan Plateau by 40 Ma, but 100 molecular-clock papers have linked supposed recent uplift to young node ages. *Journal of Biogeography*, **43**, 1479–1487.

Rosenberg NA (2004) DISTRUCT: a program for the graphical display of population structure. *Molecular Ecology Notes*, **4**, 137–138.

Royden LH, Burchfiel BC, Van Der Hilst RD (2008) The geological evolution of the Tibetan Plateau. *Science*, **321**, 1054–1058.

Sang T, Crawford D, Stuessy T (1997) Chloroplast DNA phylogeny, reticulate evolution, and biogeography of *Paeonia* (Paeoniaceae). *American Journal of Botany*, **84**, 1120–1136.

Shaw J, Lickey EB, Schilling EE, Small RL (2007) Comparison of whole chloroplast genome sequences to choose noncoding regions for phylogenetic studies in angiosperms: the tortoise and the hare III. *American Journal of Botany*, **94**, 275–288.

Shepard DB, Burbrink FT (2009) Phylogeographic and demographic effects of Pleistocene climatic fluctuations in a montane salamander, *Plethodon fourchensis*. *Molecular Ecology*, **18**, 2243–2262.

Shi YF, Li JJ, Li BY (1998) *Uplift and Environmental Changes of Qinghai-Tibetan Plateau in the late Cenozoic*. Guangdong Science and Technology Press, Guangzhou, China.

Spicer RA, Harris NB, Widdowson M (2003) Constant elevation of southern Tibet over the past 15 million years. *Nature*, **421**, 622–624.

Steinkellner H, Fluch S, Turetschek E (1997) Identification and characterization of (GA/CT)n microsatellite loci from *Quercus petraea*. *Plant Molecular Biology*, **33**, 1093–1096.

Su T, Adams JM, Wappler T *et al.* (2015) Resilience of plant-insect interactions in an oak lineage through Quaternary climate change. *Paleobiology*, **41**, 174–186.

Sun BN, Wu JY, Liu YSC (2011) Reconstructing Neogene vegetation and climates to infer tectonic uplift in western Yunnan, China. *Palaeogeography, Palaeoclimatology, Palaeoecology*, **304**, 328–336.

Sun M, Su T, Zhang SB, Li SF, AnberreeLebreton J, Zhou ZK (2015) Variations in leaf morphological traits of *Quercus guyavifolia* (Fagaceae) were mainly influenced by water and ultraviolet irradiation at high elevations on the Qinghai-Tibet Plateau, China. *International Journal of Agriculture and Biology*, **43**, 1126–1133.

Tajima F (1989) Statistical method for testing the neutral mutation hypothesis by DNA polymorphism. *Genetics*, **123**, 585–595.

Takhtajan AL (1969) *Flowering Plants: Origin and Dispersal*. Smithsonian Institution, Washington, DC.

Tao JR (2000) *The Evolution of the Late Cretaceous-Cenozoic Floras in China*, pp. 282. Science Press, Beijing, China.

Tapponnier P, Xu ZQ, Roger F *et al.* (2001) Oblique stepwise rise and growth of the Tibet Plateau. *Science*, **294**, 1671–1677.

Wang H, Qiong LA, Sun K *et al.* (2010) Phylogeographic structure of *Hippophae tibetana* (Elaeagnaceae) highlights the highest microrefugia and the rapid uplift of the Qinghai-Tibetan Plateau. *Molecular Ecology*, **19**, 2964–2979.

Wen J, Zhang JQ, Nie ZL, Zhong Y, Sun H (2014) Evolutionary diversifications of plants on the Qinghai-Tibetan Plateau. *Frontiers in Genetics*, **5**, 4.

Wu ZY, Wu SG (1998) A proposal for a new floristic kingdom (realm): the E. Asiatic Kingdom, its delineation and characteristics. In: *Floristic Characteristics and Diversity of East Asian Plants: Proceedings of the First International Symposium of Floristic Characteristics and Diversity of East Asian Plants* (eds Zhang AL, Wu SG), pp. 3–42. Springer Verlag/Higher Education Press, Beijing, China.

Wu ZY, Zhu YC, Jiang HQ (1987) *The Vegetation of Yunnan*. Science Presee, Beijing.

Wu ZH, Hu DG, Ye PS, Zhou CJ (2007) Geological evidences for the Tibetan Plateau uplifted in Late Oligocene. *Acta Geologica Sinica*, **81**, 577–587.

Xu T, Abbott RJ, Milne RI *et al.* (2010) Phylogeography and allopatric divergence of cypress species (*Cupressus* L.) in the Qinghai-Tibetan Plateau and adjacent regions. *BMC Evolutionary Biology*, **10**, 194.

Xu J, Deng M, Jiang XL, Westwood M, Song YG, Turkington R (2015) Phylogeography of *Quercus glauca* (Fagaceae), a dominant tree of East Asian subtropical evergreen forests, based on three chloroplast DNA interspace sequences. *Tree Genetics & Genomes*, **11**, 1–17.

Yin A, Harrison TM (2000) Geologic evolution of the Himalayan-Tibetan orogen. *Annual Review of Earth and Planetary Sciences*, **28**, 211–280.

Yu Y, Harris AJ, Blair C, He XJ (2015) RASP (Reconstruct Ancestral State in Phylogenies): a tool for historical biogeography. *Molecular Phylogenetics and Evolution*, **87**, 46–49.

Zachos JC, Dickens GR, Zeebe RE (2008) An early Cenozoic perspective on greenhouse warming and carbon-cycle dynamics. *Nature*, **451**, 279–283.

Zhang YL, Li BY, Zheng D (2002) A discussion on the boundary and area of the Tibetan Plateau in China. *Geographical Research*, **21**, 1–10.

Zhang SB, Zhou ZK, Hu H, Xu K (2007) Gas exchange and resource utilization in two alpine oaks at different altitudes in the Hengduan Mountains. *Canadian Journal of Forest Research*, **37**, 1184–1193.

Zhao JL, Xia YM, Cannon CH, Kress WJ, Li QJ (2015) Evolutionary diversification of alpine ginger reflects the early

uplift of the Himalayan-Tibetan Plateau and rapid extrusion of Indochina. *Gondwana Research*, **32**, 232–241.
Zhou ZK (1993) The fossil history of *Quercus*. *Acta Botanica Yunnanica*, **15**, 21–33.
Zhou ZK, Wilkinson H, Wu ZY (1994) Taxonomical and evolutionary implications of the leaf anatomy and architecture of *Quercus* L. subgenus *Quercus* from China. *Cathaya*, **7**, 1–34.
Zhou ZK, Pu CX, Chen WY (2003) Relationships between the distributions of *Quercus* Sect. *Heterobalanus* (Fagaceae) and uplift of Himalayas. *Advance in Earth Science*, **18**, 884–890.
Zhou ZK, Yang QS, Xia K (2007) Fossils of *Quercus* sect. *Heterobalanus* can help explain the uplift of the Himalayas. *Chinese Science Bulletin*, **52**, 238–247.

Z.-K.Z. planned and designed the research. H.-H.M. and X.-Y.G. performed experiments and analysed data, X.-L.J. analysed data, and H.-H.M., T.S., X.-Y.G., J.L. and Z.-K. Z. wrote the manuscript.

Data accessibility

All the sequences were deposited as GenBank (Accession nos KU245764–KU245923 and KY249208–KY249239); the nuclear microsatellite data, as well as the population localities of species distribution model, are available from Dryad Digital Repository, https://doi.org/10.5061/dryad.s7q82.

Supporting information

Additional supporting information may be found in the online version of this article.

Fig. S1 The network of genealogical relationships among the 31 haplotypes.

Fig. S2 Bayesian clustering results of the STRUCTURE analysis for nSSR data of all *Quercus* sect. *Heterobalanus* individuals from 56 populations.

Fig. S3 Distribution of the number of pairwise nucleotide differences for cpDNA of *Quercus* sect.